CHARACTERIZATION OF CONNEXIN 26 MUTATIONS CAUSING HEREDITARY SKIN DISORDERS

A Thesis Submitted to
the Graduate School of Engineering and Sciences of
İzmir Institute of Technology
in Partial Fulfillment of the Requirements for the Degree of

MASTER OF SCIENCE

in Molecular Biology and Genetics

by
Veysel BAY

June 2013
İZMİR

We approve the thesis of **Veysel BAY**

Examining Committee Members

_____
Assist. Prof. Dr. Gülistan MEŞE ÖZÇİVİCİ
Department of Molecular Biology and Genetics,
İzmir Institute of Technology

_____
Assist. Prof. Dr. Özden YALÇIN ÖZUYSAL
Department of Molecular Biology and Genetics,
İzmir Institute of Technology

_____
Assist. Prof. Dr. Engin ÖZÇİVİCİ
Department of Mechanical Engineering,
İzmir Institute of Technology

16 July 2013

_____
Assist. Prof. Dr. Gülistan MEŞE ÖZÇİVİCİ
Supervisor, Department of Molecular Biology and Genetics, İzmir Institute of Technology

_____
Assoc. Prof. Dr. Ahmet KOÇ
Head of the Department of Molecular Biology and Genetics

_____
Prof. Dr. R. Tuğrul SENGER
Dean of the Graduate School of Engineering and Sciences

ACKNOWLEDGEMENTS

I would like to express my deepest appreciation and thanks to my supervisor Assist. Prof. Dr. Gülistan MEŞE ÖZÇİVİCİ for her patience, encouragement, understanding, guidance and excellent support during my graduate studies.

Furthermore, I would like to thank to Assist. Prof. Dr. Engin ÖZÇİVİCİ, Assist. Prof. Dr. Özden YALÇIN ÖZUYSAL, Assoc. Prof. Dr. Devrim PESEN OKVUR for their helps and all graduate and undergraduate students in these three laboratories for a great working and social environment.

I would like to also thank to Assoc. Prof. Dr. Ahmet KOÇ, Assist. Prof. Dr. Çağlar KARAKAYA and Assist. Prof. Dr. Alper ARSLANOĞLU for allowing me to use their laboratory resources.

I would like to thank to especially Berrin ÖZDİL for her love, sweetness, support and patience.

I am also grateful to my parents for their infinite confidence and support all over my life.

ABSTRACT

CHARACTERIZATION OF CONNEXIN 26 MUTATIONS CAUSING HEREDITARY SKIN DISORDERS

Connexins (Cx) are building blocks of gap junctions that provide intercellular communication between adjacent cells. There exist 21 types of connexins in human body which are important for human physiology. Hence, in any case of deficiency or mutation, disorders can occur. For instance, most of the characterized Cx26 mutations are related to deafness; while there are few mutations associated with different skin disorders. One of them is a rare congenital skin disorder; Keratitis-Ichthyosis-Deafness (KID) syndrome.

In this study, we aimed to investigate the effects of Cx26 mutations associated with KID syndrome in two gap junctional communication-deficient cell lines; mouse neuroblastoma (N2A) and human cervix carcinoma (HeLa), and also in human keratinocytes (HaCaT). For this purpose, newly identified KID syndrome mutations, A88V, D50A, D50Y, and I30N were characterized. Studies on N2A cells demonstrated that Cx26 mRNA levels of mutants were higher than Cx26 WT, whereas their protein expression were very low compared to Cx26 WT. Moreover, in HeLa cells, mutant proteins were observed to be localized mainly in the cytoplasm. Furthermore, the uptake of fluorescent dyes into the cells through the mutant hemichannels was statistically higher than Cx26 WT hemichannels. For HaCaT cells, mutant proteins did not have any effect on Keratin 10 expression, a marker for suprabasal layers of epidermis. In conclusion, all four mutations caused increased hemichannel activity similar to other analyzed KID syndrome mutations, which provides a further support for the presence of increased hemichannel activity as a mechanism for mutations leading to KID syndrome.

ÖZET

KALITSAL DERİ HASTALIKLARINA SEBEP OLAN KONNEKSİN 26 MUTASYONLARININ KARAKTERİZASYONU

Konneksinler komşu hücreler arası iletişim kanalları olan oluklu bağlantıların yapı taşlarıdır. İnsan vücudunda 21 çeşit konneksin bulunmaktadır ve bunlar insane fizyolojisi için önemlidir. Bu yüzden bu genlerin eksikliğinde veya mutasyonlu durumlarda hastalıklar ortaya çıkabilir. Örneğin, Cx26 genindeki mutasyonların genellikle kalıtsal duyu kaybına neden olduğu belirlenmiştir. Ama bazı Cx26 mutasyonları deri hastalıklarına da yol açmaktadır. Bunlardan biri ırsi ve nadir bir deri hastalığı olan Keratit-İktiyozis-Sağırlık (KID) sendromudur.

Bu çalışmada, amacımız KID sendromuyla ilgili olan mutasyonların etkilerini iletişim eksiği olan iki çeşit hücre hattı; fare nöroblastoma (N2A), insan servikal karsinoma (HeLa), ve insan keratinosit hücreleri (HaCaT) kullanarak araştırmaktır. Bunun için KID sendromunda yeni tespit edilen Cx26 geni üzerindeki A88V, D50A, D50Y, ve I30N mutasyonları kullanıldı. N2A hücrelerindeki çalışmalarda mutasyonlu durumlarda Cx26 mRNA miktarlarının normale gore daha fazla; buna karşın mutant protein miktarlarının normale göre daha az olduğu gözlemlendi. HeLa hücrelerinde yapılan immunohistokimyasal çalışmalarda, mutant proteinlerin genellikle sitoplazmada lokalize olduğu gözlendi. Floresan boyalarla yapılan boya alım deneylerinde, boya alımının mutasyonlu yarımkanalların normal kanallardan istatistiksel olarak yüksek oldukları gözlemlendi. HaCaT hücreleriyle yapılan deneylerde mutasyonlu Cx26 proteinlerinin suprabasal epidermal hücrelerin markörlerinden biri olan Keratin 10 geninin ifade miktarını değiştirmediği gözlemlendi. Sonuç olarak, A88V, D50A, D50Y ve I30N mutasyonlarının KID sendromunda görülen analiz edilmiş diğer mutasyonlar gibi artan yarımkanal aktivitesine yol açtığı belirlendi. Bu da yarımkanal aktivitesindeki artışın KID sendromuna yol açan mutasyon mekanizmalarından biri olduğunu gösterdi.

TABLE OF CONTENTS

LIST OF FIGURES

Figure **Page**

LIST OF TABLES

Table **Page**

CHAPTER 1

INTRODUCTION

1.1. Gap Junctions and Connexins

Communication between cells is necessary to coordinate the cellular activities and provide the tissue homeostasis in multicellular organisms for cell growth, differentiation and development. In order to communicate with each other, cells use gap junctions that provide a direct linkage between the cytoplasm of neighboring cells. Gap junction channels consist of two apposed hexameric connexin (Cx)-assembled pores in vertebrates, or innexin-assembled pores in invertebrates (Goodenough and Paul, 2009). Gap junctional intercellular communication (GJIC) enables the transfer of molecules smaller than 1 kDa such as secondary messengers (IP_3), metabolites (ATP), and ions (Ca^{2+}) between adjacent cells (Scott and Kelsell, 2011).

To date at least 21 members of the connexin protein family have been identified in the human genome. The nomenclature of connexins is based on either the molecular mass, or structure and sequence homology of the particular connexin of interest. In case of classification based on molecular weight, connexins are referred as connexin with their molecular weight. For instance, Cx43 is a protein with a molecular weight of 43 kDa, similarly the molecular weight of Cx26 protein is 26 kDa. Moreover, connexins are classified according to their structural and sequence homology as α-, β-, γ -, δ-, and ε-Cxs. For instance, Cx43 and Cx40 belong to α-Cxs, Cx26 and Cx30 belong to β-Cxs (Scott and Kelsell, 2011). For this reason, α-connexins are named as gap junction α (*GJA*) proteins, β-connexins are named as gap junction β (*GJB*) proteins, and γ-connexins are named as gap junction γ (*GJC*) proteins, in this classification for example *GJA1* refers to Cx43 and *GJB2* refers to Cx26 (Kelsell et al., 2001).

Gap junction channel assembly starts with oligomerization of six connexins into hemichannels/connexons. Connexons are then transferred to the plasma membrane where they can either function by themselves as hemichannels or align with another connexon from a neighboring cell to complete the formation of gap junctions. The types of both hemichannels and intercellular junctions vary depending on the connexins

contributing the channel formation. Hemichannels that are formed by the same connexin types are called homomeric hemichannels, however when they are formed by different connexins they are called heteromeric hemichannels. If both hemichannels have the same connexin compositions either homomeric or heteromeric, these gap junctions are called homotypic, but if they have different connexon compositions they are called heterotypic gap junctions (Figure 1.1), (Meşe et al., 2007, Lee and White, 2009).

In general, connexins can form functional heteromers with connexins in the same subgroup. Furthermore, they can also be compatible to connexins in other subgroups. For instance, Cx26 (β) can form heteromeric hemichannels with Cx32 (β) but not with Cx43 (α). On the other hand, Cx36 (α) is compatible with Cx45 (γ) to form functional gap junction channels. These indicate that, there is a complex relationship between connexins during heteromeric hemichannel and intercellular channel formation, but the mechanism of the compatibility of connexins is not exactly known (Gemel et al., 2004).

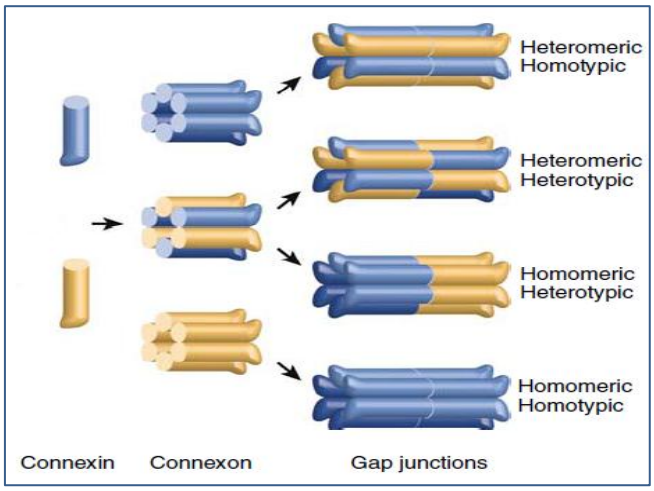

Figure 1.1. Assembly of gap junctions: Homomeric and heteromeric connexons are formed by connexin proteins and these connexons form homotypic or heterotypic gap junctions at the plasma membrane (Source: Meşe et al., 2007).

1.2. Structure of Connexins

Connexin proteins have four transmembrane domains, one N-terminus, one C-terminus, two extracellular loops, and one cytoplasmic loop between the second and the third transmembrane domains (Figure 1.2). Transmembrane domains form the walls of channel and they are connected with each other through extracellular loops. On

extracellular loops there are highly conserved disulfide bonds that play role in hemichannel recognition and docking, as well as the assembly of functional gap junction channels. In addition to transmembrane domains, these extracellular loops are also highly conserved in connexin protein family. The uniqueness of connexins results from the differences in their cytoplasmic loop and C-termini sequences and lengths. C-terminus and cytoplasmic loop are also the post-translational modification sites and they are the regulation sites for connexins. For instance C-terminus of Cx43 is highly phosphorylated, whereas C-terminus of Cx26 that is very short compared to other connexins is not phosphorylated (Laird, 2005). N-terminus of connexins is also conserved among connexin protein family (Meşe et al., 2007).

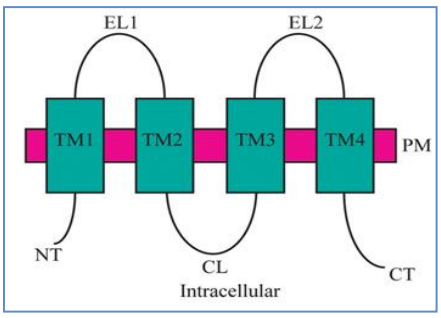

Figure 1.2. Connexin protein structure: Connexins have four transmembrane domains, two extracellular loops, one cytoplasmic loop, one N-terminus and one C-terminus (Source: Scott and Kelsell, 2011).

1.3. Turnover of Connexin Proteins

In eukaryotic cells, transmembrane proteins are produced in ER-bound ribosomes and transferred to the Golgi apparatus then transported to the plasma membrane. Connexins are inserted into the ER membrane during translation. Then six connexins are oligomerized in the ER-Golgi intermediate compartment (ERGIC), or trans-Golgi region depending on the connexin subtype. For instance, Cx32 and Cx26 are oligomerized in ERGIC, but Cx43 is oligomerized in the trans-Golgi region (Koval, 2006). Connexins form hemichannels/connexons in the trans-Golgi region. After oligomerization, they are carried to the plasma membrane on microtubules, and then inserted into the plasma membrane. In the plasma membrane, connexons can either form non-junctional hemichannels or they can laterally diffuse towards the cell-cell contact regions to align with another connexon from an adjacent cell to form a gap junction channel. Next, hundreds to thousands of intercellular channels aggregate to

assemble structures known as gap junction plaques on the plasma membrane. Connexins have a half life between 1.5-5 hours that is faster than many other cell surface proteins (Musil et al., 2000). For the degradation of connexins, they initially form cytoplasmic annular junction by internalized gap junctions that are generated by invagination, restriction, pinching-off and transport of both junctional membranes into one of the adjacent cells. Then annular junctions are transferred to lysosomes or proteasomes for degradation of connexins (Figure 1.3) (Segretain and Falk, 2004).

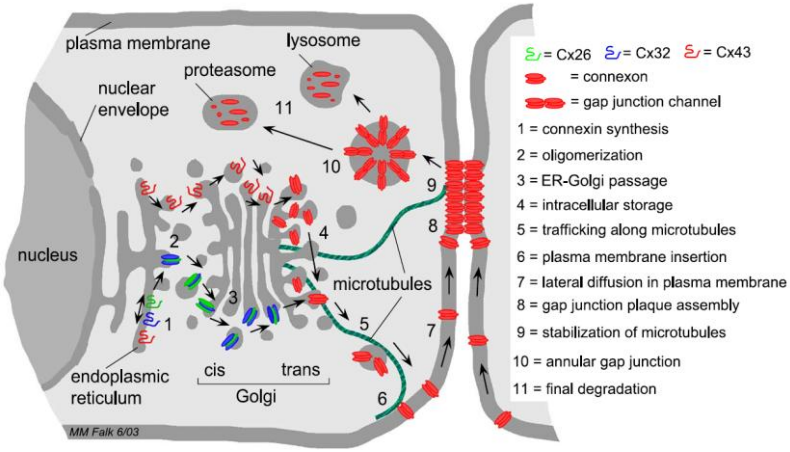

Figure 1.3. Synthesis, assembly and degradation of gap junction membrane channels: Connexins move to the plasma membrane through secretory pathway and they are degraded in lysosomes or proteasomes (Source: Segretain and Falk, 2004).

1.4. Permselectivity of Gap Junctions

Gap junctions were thought to be non-selective, passive pores that permit the free transfer of small molecules. Recent studies showed that gap junctions have selective permeability which could be inferred from the unique conductance, gating and permeability of channels that consist of different connexins. Furthermore, different connexins have been shown to be related to a variety of human disorders that also demonstrates the uniqueness of each connexin. In terms of transfer of ions such as Ca^{2+} and Na^{+}, there occur minimal changes in their selectivity among connexins. However, for transfer of larger molecules such as ATP and secondary messengers such as IP_3, different connexins have different selectivity (Meşe et al., 2007).

Gap junction channels, either homotypic or heterotypic, are voltage-dependent channels. However, the sensitivity and kinetics differ from one type to another.

Monovalent ions are not much selectively transferred in contrast to larger molecules and the sequence of monovalent cation selectivity is similar in connexin channels with different conductances (Goldberg et al., 2004). Cx32 and Cx26 were incorporated into liposomes and their permeability was investigated with radiolabeled tracers. Endogenous solutes such as cGMP, or cAMP passed uniformly through homomeric hemichannels formed by Cx32. However, cGMP transfer through heteromeric hemichannels formed by Cx32 and Cx26 was more efficient than cAMP transfer. This shows that cAMP transfer was limited by Cx26 in these heteromeric hemichannels (Bevans et al., 1998). Moreover, adenosine transfer by Cx32 was more efficient than Cx43, but when it was phosphorylated, for example in case of ATP, its transfer selectivity shifted to Cx43 rather than Cx32. As a consequence of this knowledge, Cx32 could be said to be less likely to pass negatively charged groups like phosphates, or larger molecules than Cx43 channels (Goldberg et al., 2002). However, the transfer through gap junctions is not only charge-dependent. Hela cells were transfected with Cx26, Cx32 and Cx43 and an anionic molecule, IP_3, was injected into these cells and their intracellular Ca^{2+} level changes were measured. As a result, IP_3 was more efficiently transferred by Cx32 containing channels than Cx43 or Cx26 containing channels (Niessen et al., 2000). Therefore, gap junction permeability is dependent on connexin composition, specific ionic changes and post-translational modifications e.g. phosphorylation (Zoidl and Dermietzel, 2010).

Fluorescent dyes such as Lucifer yellow (LY), ethidium bromide (EtBr), neurobiotin (NB), propidium iodide (PI) and 4',6-diamidino-2-phenylindole (DAPI) are also used to determine the presence of functional GJIC between neighboring cells. These dyes are in different sizes and have different charges. Gap junction channels show different permeability to different dyes. HeLa cells were transfected with Cx26, Cx31, Cx32, Cx37, Cx40, Cx43 and Cx45 and permeabilities of these connexins were investigated with different tracers. As a result, LY was able to pass through all connexin channels analyzed. On the other hand, EtBr and PI transfer through Cx31 and Cx32 junctions was very poor, respectively. Moreover, DAPI showed less transfer through Cx31 or Cx43 channels. In addition, NB transfer through Cx31 was very weak compared to other connexins (Elfgang et al., 1995). Furthermore, gap junctions in mouse embryonic stem cells were shown to be more permeable to a small molecule, such as NB, than larger molecules such as LY and EtBr (Wörsdörfer et al., 2008).

1.5. Physiological Significance of Connexins

Connexins are important for human physiology as a variety of human hereditary diseases have been shown to be associated with mutations in connexin genes (Laird, 2010). Connexin-linked diseases result from mutations that affect various mechanisms in the biogenesis and the function of channels such as channel formation, channel permeability, protein expression, oligomerization, gap junjction assembly or protein localization. Most of the autosomal recessive and dominant connexin-linked disorders are associated with single missense mutations in the coding regions of connexin genes. At least 10 disorders have been shown to be caused by connexin mutations. For example, 40-50 % of inherited neurosensory disorder cases are caused by mutations in the genes of Cx26, Cx30, Cx31, Cx32 and Cx43. There are other neuropathies such as X-linked Charcot-Marie-Tooth disease (CMTX) caused by Cx32 mutations and Pelizaeus-Merzbacher disease caused by Cx47 mutations. Furthermore, mutations in Cx26, Cx30, Cx30.3, and Cx43 are also related to various skin disorders such as Keratitis-Ichthyosis-Deafness (KID) syndrome, palmoplantar keratoderma (PPK), erythrokeratodermia variabilis (EKV), hidrotic ectodermal dysplasia (HED) and Clouston's syndrome. In addition, Cx46 and Cx50 mutations cause congenital cataracts, and Cx43 mutations cause developmental disorder oculodentodigital dysplasia (ODDD). Furthermore, Cx40 mutations cause atrial fibrillation (Table 1.1) (Laird, 2010).

Gene	Disease	Expression Pattern
GJB2 (Cx26)	Deafness (OMIM; 220290 and 601544) **Keratitis-Ichthyosis-Deafness syndrome (OMIM; 148210)** Vohwinkel Syndrome (OMIM; 604117) Palmoplantar keratoderma with deafness (OMIM; 144200) Hystrix-like ichthyosis–deafness syndrome (OMIM; 602540)	**Cochlea** **Skin** Liver Placenta Breast
GJA1 (Cx43)	ODDD (OMIM; 164200) Syndactyly, type III (OMIM; 186100) Hypoplastic left heart syndrome (OMIM; 241550) Atrioventricular septal defect (OMIM; 606215)	Most of tissues
GJB1 (Cx32)	CMT neuropathy, X-linked (OMIM; 302800)	Liver Oligodendrocytes Schwann cells
GJA8 (Cx50)	Cataract (OMIM; 116200)	Lens
GJB3 (Cx31)	Erythrokeratodermia variabilis (133200) Deafness (OMIM; 603324)	Cochlea Skin Placenta
GJB6 (Cx30)	Deafness (604418) Clouston syndrome (OMIM; 129500)	Cochlea Skin Brain

Table 1.1. Connexin-related human disorders
(Source: modified from Zoidl and Dermietzel, 2010)

1.6. Connexin Mutations in Diseases

Different cell types can express many types of connexins at the same time. Therefore, gap junctions are formed by complex interactions of different connexins. Thus, it becomes difficult to observe the effects of each mutation on gap junction biogenesis and function. Therefore, mechanism of each mutation is studied one by one in communication-deficient cell lines to examine the effect of mutations on the biogenesis of connexins and/or channel functionality. Based on these studies, the mechanisms of connexin mutations leading to human disorders could be classified into four main groups: mutant connexin mistrafficking, dominant negative effect of mutant connexins on other connexins, loss of function, and aberrant hemichannel formation (Figure 4, Scott et al., 2011). As an example of mutant connexin mistrafficking, in moderate and severe CMTX cases; G12S, R142W, E186K and E208K mutations in Cx32 were shown to be localized to cytoplasm rather than plasma membrane. However,

in mild cases such as R15Q, V63I, V139M, and R220Stop mutant Cx32 proteins could be observed in the plasma membrane (Deschênes et al., 1997). Furthermore, EKV-linked Cx31 mutants, R42P, C86S, and G12D, were demonstrated to be trafficked to the cytoplasmic membranous structures rather than the plasma membrane (Tattersall et al., 2009). Another mechanism is dominant negative effect of mutant connexins on others. For instance, P87L and R143W mutations on Cx26 cause dominant negative effect on connexin mediated cell growth function of Cx26 WT. However, C60F mutation caused dominant negative effect on GJIC function (Dancer et al., 1997). Furthermore, mutations on one type of connexins could affect the function of other types of connexins by inhibiting their hemichannel formation or by forming heteromeric hemichannels with them. For instance, neurobiotin uptake efficiency was similar between Cx26 WT and Cx30 WT co-expressing Hela cells and Cx30 WT only expressing cells. However, when Cx30 WT is co-transfected with nonsyndromic deafness mutations, W44S and R75W in the Cx26 gene, neurobiotin uptake efficiency was significantly decreased (Marziano et al., 2003). In terms of loss of function in connexin types, 35delG on Cx26 can be given as an example that causes premature termination of the protein translation which is the cause of the majority of the nonsyndromic recessive deafness, DFNB1 (White and Paul, 1999). As an example for aberrant hemichannel function, G45E mutation in the Cx26 that is associated with KID syndrome, results in leaky hemichannels, which caused cell lysis and then cell death (Gerido et al., 2006). Moreover, N14K mutation on Cx26 that is linked to deafness and skin disorders, KID/HID syndrome, causes higher hemichannel activity than Cx26 WT (Lee et al., 2009).

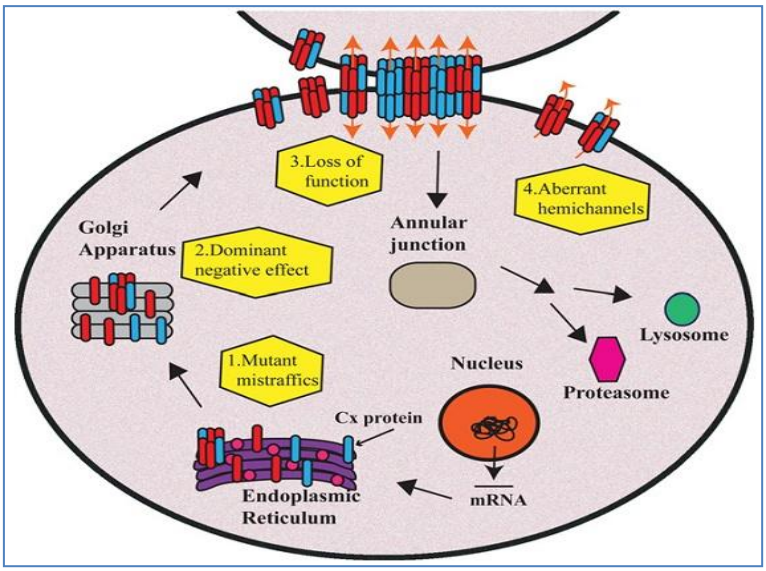

Figure 1.4. Mechanisms of disease associated mutant connexin proteins: Four main groups of disease associated mechanisms (Source: Scott and Kelsell, 2011).

1.7. Connexins in Skin

Skin consists of two layers, mesodermally derived dermis and ectodermally derived epidermis (Stelnicki et al., 1997). Epidermis is formed by four main layers, basal, spinous, granular and stratum corneum. These layers consist of keratinocytes and the cells at the basal layer migrate from the most inner layer to the stratum corneum that consists of dead corneocytes. The role of gap junction in the epidermal homeostasis is not known but connexins are thought to be important for the keratinocyte proliferation, migration, and differentiation by their roles in GJIC and some unknown GJ-independent functions.

In each layer of the skin, different connexins are expressed (Figure 1.5, Meşe et al., 2007)). In humans Cx43 is expressed in basal, spinous and granular layers. Cx26 is expressed in both basal and granular layers. Cx40 is expressed in both spinous and granular layers. Cx30.3 is only expressed in granular layer. In granular layer and at the end of spinous layer closed to granular layer Cx30, Cx31, Cx31.1, Cx37 and Cx45 are expressed. The connexin expression profile is quite different in rodents from human (Table 1.2) (Scott and Kelsell, 2011).

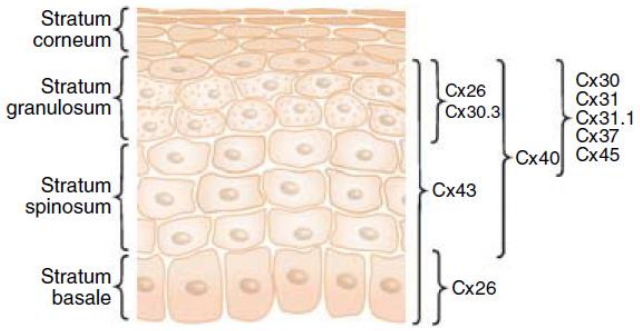

Figure 1.5. Connexin expression in adult human epidermis: Different connexins are expressed in each layer of skin (Source: Meşe et al., 2007).

	Human	Rodent
Epidermis		
Basal cell l.	Cx26; (Cx43)	Cx40; Cx43; Cx37
Spinous cell l.	Cx43>Cx31>Cx37	Cx43; Cx31; Cx31.1; Cx37; (Cx26)
Granular cell l.	Cx43>Cx31>Cx37	Cx31; Cx31.1; Cx37; (Cx26)
Hair follicle		
IRS	Cx26>Cx43	Cx31; Cx26
ORS	Cx43>Cx26	Cx43>Cx40
Sebaceous glands	Cx43	Cx31>Cx40/Cx43
Eccrine sweat glands	Cx31; Cx26 (Cx43)	Cx31; Cx26
Dermal fibroblasts	Cx43; Cx40	Cx43

Table 1.2. The connexins expressed in human and rodent skins (Source: Richard G., 2000)

1.8. Keratitis-Ichthyosis-Deafness (KID) Syndrome

Keratitis-Ichthyosis-Deafness (KID) syndrome is a congenital rare autosomal disorder. It causes vascularizing keratitis with hyperkeratotic skin lesions, ichthyosis with a fish scale appearance, and hearing loss. The reason of KID syndrome is dominant mutations in Cx26 gene and uncommonly in Cx30 gene. It is mostly sporadic and caused by missense mutations (Jan et al., 2004, Titeux et al., 2009). Most of the patients carry distinct missense mutations in the Cx26 gene. For instance, missense mutations A40V, G45E and D50N were detected on the first extracellular loop of Cx26 in the patients with KID syndrome (Sanchez et al., 2010). D50N mutation was detected with a different novel mutation D50Y on Cx26 in Japanese patients with KID syndrome (Yotsumoto et al., 2003). Recently D50A mutation was detected in a 5-week old child with KID syndrome and Dandy-Walker malformation (Cushing et al., 2008). Moreover, A88V mutation on the second transmembrane domain was detected in a prematurely born 33-week old child with the symptoms of KID syndrome (Koppelhus et al., 2010).

Additionally, I30N mutation was detected on the first transmembrane domain of Cx26 in a 50 year old patient with KID syndrome (Arndt et al., 2010).

Most of Cx26 associated mutations result in nonsyndromic deafness without skin disorders in humans. This demonstrates that skin disorders cannot be related to loss of channel activity of Cx26 alone (Gerido and White, 2004). Besides, most of the mutations that cause hearing loss have been characterized that showed either the complete or partial loss of channel function. On the other hand, mutations for skin disorders are less characterized and needed to be studied to understand the mechanisms of the skin diseases related to these Cx26 mutations.

1.9. Aim of the Project

The aim of this project is the functional characterization of newly identified Cx26 mutations related to KID syndrome; D50A, D50Y, A88V and I30N. Hence, it will be investigated whether these mutations have similar effects to other KID syndrome associated mutations which had been observed to cause increased hemichannel activity and mistrafficking of mutant proteins.

CHAPTER 2

MATERIALS AND METHODS

2.1. Site-directed Mutagenesis of Connexin 26 Gene

Four mutations associated with KID syndrome were selected to study. In order to create mutations on the Cx26 gene human Cx26 cDNA was used as a template and primers in the Table 2.1 were designed and used in PCR reaction. A88V mutation was created by changing cytosine to thymine at the 263th position D50A mutation was created by changing adenine to cytosine at the 149th position. D50Y mutation was created by changing guanine to thymine at the 148th position. Finally, I30N mutation was created by changing thymine to adenine at the 89th position. Localization of mutations was given in Figure 2.1.

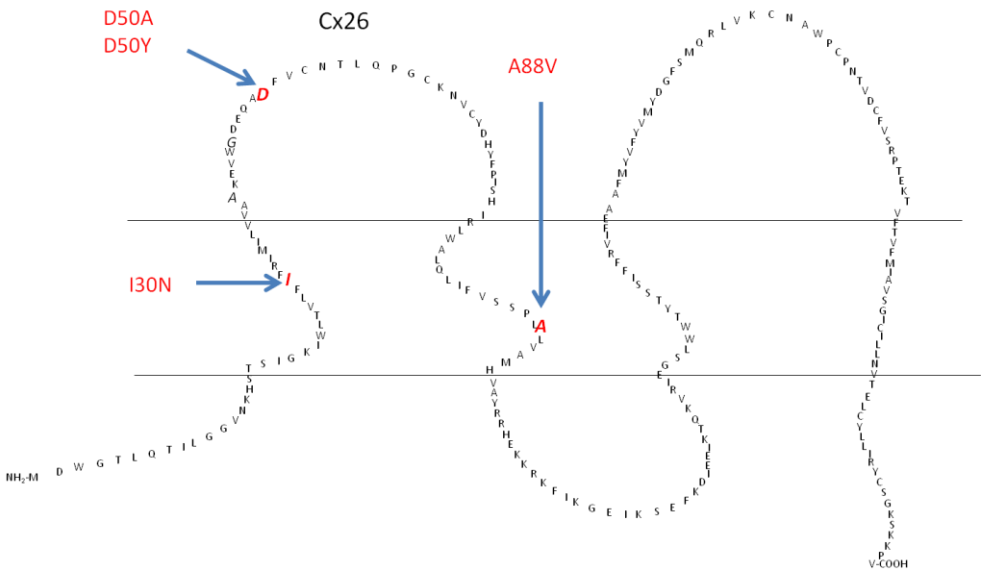

Figure 2.1. Localization of mutations on Cx26 gene: I30N is on the first transmembrane domain, D50A and D50Y are on the first extracellular loop, and A88V is on the second transmembrane domain.

Cx26 Forward Primer	5’- tgttgtggatccatggattggggcacgc-3’
Cx26 Reverse Primer	5’- tgttgtggatccttaaactggctttttt-3’
Cx26 D50A Forward Primer	5’- gatgagcaggccg**C**ctttgtctgca-3’
Cx26 D50A Reverse Primer	5’- tgcagacaaag**G**cggcctgctcatc-3’
Cx26 D50Y Forward Primer	5’- gatgagcaggcc**T**actttgtctgca-3’
Cx26 D50Y Reverse Primer	5’- tgcagacaaagt**A**ggcctgctcatc-3’
Cx26 A88V Forward Primer	5’- gtgtccacgccag**T**gctcctagtggc-3'
Cx26 A88V Reverse Primer	5’- gccactaggagc**A**ctggcgtggacac-3’
Cx26 I30N Forward Primer	5’- ccgtcctcttca**A**ttttcgcattatga-3
Cx26 I30N Reverse Primer	5’- tcataatgcgaaaa**T**tgaagaggacgg-3’

Table 2.1. Primers for wild type Cx26 and single nucleotide changes in Cx26 gene. Nucleotide changes are shown with capital letters on primers.

Cx26 forward and reverse primers were designed with BamHI restriction sites and six inert bases to prevent loss of restriction sites during digestion reactions. Other primers were designed with the single base changes to create mutations at the desired sites (shown in bold in the Table 2.1). In order to generate the mutant Cx26 gene, three PCR reactions were set up. Initially, by using Cx26 forward primer and the reverse primer for the mutation of interest, the first PCR product was produced (5’ mutant DNA piece). Similarly, by using Cx26 reverse primer and the forward primer for the same mutation, second PCR product was produced (3’ mutant DNA piece). Finally, to produce the whole Cx26 gene with the desired mutations the first and second PCR products were used as a template in the last PCR reaction together with Cx26 forward and reverse primers (Figure 2.2).

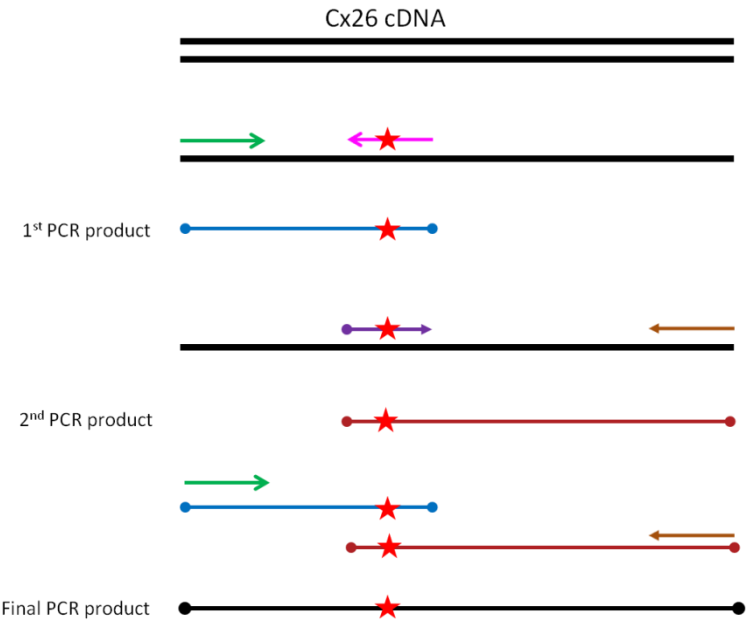

Figure 2.2. Site-directed mutagenesis for Cx26 cDNA. Star sign refers to the locations of altered nucleotides.

2.2. Preparation of Competent Bacteria

E. coli JM109 cells were inoculated into Luria Broth (LB) agar with a bacterial loop to get single colonies and they were grown at 37 °C for 16 hours. The following day a single colony was inoculated into 2 ml LB medium and it was incubated at 37 °C, shaking at 250 rpm overnight. Then, bacteria in the LB medium were diluted 100 fold in LB medium and was incubated at 37 °C, 250 rpm until the OD was between 0.3 and 0.6 at 600 nm. Cells were centrifuged at 5000 rpm at +4 °C for 10 minutes. Bacterial pellet was resuspended in 50% LB medium and 50% 2X TSS (10 % polyethylene glycol, 5 % dimethyl sulfoxide, 20 mM $MgCl_2$ in LB) buffer. Finally they were flash frozen with liquid nitrogen and kept at -80 °C in small aliquots.

2.3. Cloning of PCR Products into pBSBK Cloning Vector

After creating Cx26 PCR products with mutations, they were cloned into bacterial cloning vector pBSBK. pBSBK and PCR products were cut with BamHI enzyme (NEB) and controlled on agarose gel. The digested pieces were isolated from agarose gel by Sigma GenElute Gel Extraction Kit (Cat# NA1111). Isolated pBSBK DNA was treated with alkaline phosphatase (AP), CIAP (NEB) in order to prevent self ligation. After that

vector and Cx26 inserts were ligated with T4 DNA ligase (NEB) at 16 °C overnight. On the following day, ligation mixtures were transformed into competent *E. coli* JM109 bacteria with heat-shock and bacteria were inoculated into ampicillin containing LB-agar plates. Single colonies were grown overnight in 2 ml LB medium with ampicillin overnight and plasmid isolation was done with miniprep method using TENS buffer (10 mM Tris-HCl pH 8.0, 1 mM EDTA pH 8.0, 0.1 N NaOH, 0.5 % SDS). To verify the insertion of the PCR products, isolated plasmids were cut with BamHI to observe the presence of pBSBK vector and Cx26 inserts on agarose gel. Positive colonies with the plasmid were grown in 50 ml LB medium for DNA isolation with Sigma GenElute Plasmid Midiprep Kit (PLD35) Purified vectors were sent to Macrogen Inc. for sequencing to verify the location and the presence of mutations.

2.4. Subcloning of Cx26 Mutants into pIRES2-EGFP and pIRES2-DsRed2 Mammalian Expression Vectors

pIRES2-EGFP and pIRES2-DsRed2 vectors were cut with BamHI enzyme and run on agarose gel. Digested vectors were isolated from the gel, and then were AP-treated. Meanwhile, purified pBSBK-Cx26 clones were digested with BamHI enzyme and mutant Cx26 inserts were purified from agarose gel. Then, Cx26 inserts were ligated into AP-treated pIRES2-EGFP and pIRES2-DsRed2 vectors with T4 DNA ligase overnight. Then, transformations of ligation mixtures into *E. coli* JM109 bacteria were done with heat-shock method and were spread onto LB plates with kanamycin. Colonies were grown overnight in 2 ml LB medium with kanamycin for plasmid isolation. Isolated plasmids were cut with BamHI and run in agarose gel for the verification of inserts in the vectors. In order to determine the correct orientation of Cx26 inserts into the vectors correct plasmids were cut with ApaI enzyme and run on agarose gel. Correctly inserted clones were prepared with a midiprep isolation kit.

2.5. Maintenance of HeLa, N2A and HaCaT Cells

Human cervical carcinoma HeLa cells were grown in low glucose containing DMEM (Hyclone, Cat#SH30021.01) with 10 % fetal bovine serum (FBS) (Biological Industries, Cat#716684) and 1 % penicillin/streptomycin (invitrogen, Cat#1092595).

Mouse neuroblastoma N2A cells were grown in high glucose containing DMEM (Hyclone, SH30022.01) with 10 % FBS and 1 % penicillin/streptomycin.

While passaging both HeLa and N2A cells, 0.25 % trypsin/EDTA solution (Biological Industries, Cat#03-052-1B) was used.

Immortalized human keratinocyte HaCaT cells were grown in high modified DMEM (Hyclone, SH30285.01) with 2mM L-glutamine, 10 % FBS and 1 % penicillin/streptomycin. While passaging, HaCaT cells were incubated with 0.05 % EDTA solution (Biological Industries, Cat#03-015-1B) at 37 °C, 5% CO_2 for about 20 minutes to disrupt the desmosome structures between connecting cells. Then they were lifted up with 0.05 % trypsin/0.025 % EDTA (Biological Industries).

2.6. Transfection of Cx26-pIRES2-EGFP and pIRES2-DsRed2 Constructs into N2A, HeLa and HaCaT Cells

HeLa, N2A and HaCaT cells were transfected with Cx26 WT and mutant clones for functional analysis. For HeLa and N2A cells transfection was performed with Lipofectamine 2000 transfection reagent (Invitrogen, Cat#11668-019) using 1 µg DNA per 2 µl Lipofectamine. For HaCaT cells transfection was performed using Fugene HD transfection reagent (Promega, Cat#E2311) using 1 µg DNA per 3 µl Fugene. Media of HeLa and N2A cells were changed 6 hours after transfection in order to prevent toxic effects of Lipofectamine 2000. The media of HaCaT cells was changed 24 hours after transfection. In both cases, 3.2 mM $CaCl_2$ was added into the media 6 hours after transfection to prevent the probable aberrant hemichannel activity of mutant Cx26 proteins.

2.7. Immunohistochemistry of Cx26 in HeLa Cells

HeLa cells grown on cover-slips were transfected with pIRES2-EGFP constructs. The transfection efficiency was controlled under the fluorescent microscope on the following day. The media of cells were aspirated and cells were washed with 1X PBS. Cells were fixed with 4 % Paraformaldehyde (PFA) for 10 min at room temperature. After rinsing three times with 1X PBS, cells were permeabilized with 0.1 % TritonX-100/1X PBS for 15 minutes at room temperature, followed by blocking with 3 % BSA (Amresco, Cat#0332-1006) in 0.1 % TritonX-100/1X PBS (blocking solution) for 30 minutes at room temperature. Cells were incubated with the rabbit anti-Cx26 antibody (1:500), (Invitrogen, Cat#51-2800) in blocking solution for 1 hour at room temperature. Antibody-treated cells were washed with 1X PBS. Then, cells were incubated with Alexa555-conjugated goat anti-rabbit secondary antibody (1:200) (Invitrogen, Cat#A21428). Following secondary antibody treatment cells were incubated with 300 nM DAPI/1X PBS for 5 minutes at dark. After washing cells with 1X PBS at dark, cover-slips were dipped in ddH_2O, dried shortly and mounted on slides with DABCO (Sigma, Cat#BCBH2276V) mounting medium at dark. Pictures of cells were taken under fluorescent microscope with 40X magnification.

2.8. Protein Isolation from N2A Cells

Transfected N2A cells were flash frozen in liquid nitrogen and stored at -80 °C. For protein isolation frozen cells were thawed on ice for 5 minutes. Lysis buffer (10 mmol/l Tris pH 7.5, 1 mmol/l EDTA, 0.1 % Triton X-100, 1X protease inhibitor and 1 mM DTT) was added on the cells and the cells were scraped with a cell lifter. Lysates were collected into 1.5 ml Eppendorf tubes and were homogenized with an insulin syringe for 5-10 times. Then, the lysates were incubated on ice for 20 minutes. After incubation they were briefly vortexed and spun at 14000 rpm, at +4 °C for 10 minutes. Supernatants that contain proteins were transferred into fresh Eppendorf tubes and stored at -80 °C.

2.9. Bradford Assay

Isolated proteins were 1:200 diluted with 1 µl protein, 159 µl dH_2O and 40 µl 5X Bradford reagent in a 96-well plate as two replicates. Then, their concentrations were measured in spectrophotometer at 595 nm with a range of BSA calibrator concentrations 0.2, 0.5, 1, 2, 4, 8 mg/ml.

2.10. Western Blotting

Isolated proteins were prepared with 5x Loading dye and dH_2O to 40 µg final concentrations. Then, they were run on SDS gel that consists of 15 % resolving gel and 3 % stacking gel with protein marker (NEB) in 1X running buffer. They were run at 200 V until marker was clearly separated.

SDS gel and nitrocellulose membrane were soaked in 1X transfer buffer and proteins were transferred to nitrocellulose membrane in 1X transfer buffer at 250 mA for two hours. After two hours membrane was rinsed with 1X TBS-Tween-20 (0.05 %) (TBS-T) and blocked with 5 % milk powder in 1X TBS-T (blocking solution) for 1 hour. After blocking membrane was incubated with rabbit anti-Cx26 (invitrogen) primary antibody that was 1:1000 diluted in the blocking solution, overnight at 4 °C. The following day, membrane was rinsed with 1X TBS-T for 15 minutes three times. Then, the membrane was incubated with peroxidase conjugated goat anti-rabbit secondary antibody (Pierce, Cat#31460) that was 1:2500 diluted in blocking solution, at room temperature for 2 hours. After that membrane was washed with 1X TBS-T for 20 minutes once and 10 minutes twice.

Membrane was incubated with SuperSignal West Pico Chemiluminescent Substrate (Thermo) and visualized in Versadoc imaging system (Biorad) in Izmir Institute of Technology, Biotechnology and Bioengineering Research and Application Center. After visualization, densities of Cx26 bands were measured. In addition, the same procedure was applied to γ-tubulin expression as a loading control by using mouse anti-γ-tubulin as a primary (Sigma, 070M4856) (1:10000) and goat anti-mouse as a secondary (1:1000) (Dako, 00071312) antibodies. After visualization densities of γ-tubulin bands were also measured.

2.11. RT-PCR of Cx26

Total RNA isolation from N2A cells and HaCaT cells was performed by using PureLink® RNA Mini Kit following the manufacturer's protocol (invitrogen, 12183018). Isolated RNAs were used for cDNA synthesis by Fermentas First Strand cDNA Synthesis Kit (Thermo, K1622) using random hexamers.

For N2A cells, expression of Cx26 gene was analyzed by using human Cx26 primers and control, mouse GAPDH, primers (Table 2.2).

For HaCaT cells expression of Cx26 and Keratin10 genes were analyzed with human Cx26 and human Keratin10 primers. For control human GAPDH primers were used (Table 2.2)..

RT-PCR was done in BioRad IQ5 & MYQ system. Analysis of RT-PCR results was performed by Delta-Delta Ct method.

Cx26 Forward Primer	5'-ctgcagctgatcttcgtgtc-3'
Cx26 Reverse Primer	5'-aagcagtccacagtgttg-3'
Keratin 10 Forward Primer	5'-gccaacatcctgcttcagat-3'
Keratin 10 Reverse Primer	5'-ggctctcaatttgcatctcc-3'
humanGAPDH Forward Primer	5'-gaaggtgaaggtcggagtca-3'
humanGAPDH Reverse Primer	5'-aatgaaggggtcattgatgg-3'
mouseGAPDH Forward Primer	5'-gacatgccgcctggagaaac-3'
mouseGAPDH Reverse Primer	5'-agcccaggatgccctttagt-3'

Table 2.2. Primers used in RT-PCR for N2A and HaCaT cells

2.12. Dye Uptake

In gap junction experiments fluorescent dyes are used to determine the presence of functional GJIC. These dyes could be in different sizes and have different charges. In this study neurobiotin (NB) which has 287 Da molecular mass and +1 charge; ethidium bromide (EtBr) which has 394 Da molecular mass and +1 charge; and Lucifer yellow (LY) which has 433 Da molecular mass and -2 charge were used (Wörsdörfer et al., 2008).

2.13. Ethidium Bromide (EtBr) Uptake Assay

Cells were transfected with pIRES2-EGFP constructs and incubated for 24 hours in the presence of 3.2 mM $CaCl_2$. Following day cells were incubated in Ca^{2+}-free medium for 20 minutes at 37 °C, 5% CO_2. After that cells were washed with 1X PBS. Next, cells were incubated with 10 µM EtBr-1X PBS for 3 minutes at room temperature and then cells were washed with 1X PBS containing 3.2 mM $CaCl_2$ for three times. Next, cells were fixed with 4 % PFA for 10 minutes. After washing cells with 1X PBS three times for 10 minutes, cells were observed under the fluorescent microscope and images were taken for analysis.

2.14. Lucifer Yellow (LY) Uptake Assay

Cells were transfected with pIRES2-DsRed2 constructs. 24 hours after transfection cells were incubated in Ca^{2+}-free medium for 20 minutes at 37 °C, 5% CO_2. Then cells were washed with 1X PBS. After that cells were incubated with 2.5 mg/ml Lucifer Yellow in 1X PBS for 20 minutes. After 20 minutes cells were washed with 1X PBS with 3.2 mM $CaCl_2$ three times for 10 minutes. After fixing with 4 % PFA for 10 minutes, cells were washed with 1X PBS three times and finally they were washed with 1X PBS and observed under fluorescent microscope. Images were taken for analysis.

2.15. Neurobiotin (NB) Uptake Assay

Cells were transfected with pIRES2-EGFP constructs and incubated for 24 hours in the presence of 3.2 mM $CaCl_2$. Following day cells were incubated in Ca^{2+}-free medium for 20 minutes at 37 °C, 5% CO_2. Then cells were washed with 1X PBS containing 3.2 mM $CaCl_2$ three times for 10 minutes. After that, cells were incubated with 0.5 mg/ml NB-1X PBS at room temperature and then cells were washed with 1X PBS that contains 3.2 mM $CaCl_2$ for three times. Next, cells were fixed with 4 % PFA for 10 minutes, permeabilized with 0.1 % TritonX-100-1X PBS for 10 minutes, blocked with 3 % BSA-0.1 % TritonX-100-1X PBS for 15 minutes. Then, cells were incubated with tetra methyl rhodamine isothiocyanate (TRIT-C) conjugated streptavidin that was

1:1000 diluted in 3 % BSA-0.1 % TritonX-100-1X PBS for 30 minutes at dark. Finally cells were washed with 1X PBS and observed under fluorescent microscope. Images were taken for analysis.

Analysis was done by using ImageJ program with thresholding method; Moments, threshold color; black and white (B&W), and color space; red-green-blue (RGB). For EtBr and NB uptake assays only the passage of red was allowed and red histogram was chosen. However, for LY uptake assay only the passage of green was allowed and green histogram was chosen.

CHAPTER 3

RESULTS

3.1. Cloning of Mutant Cx26 genes

KID syndrome associated mutations; A88V, D50A, D50Y, and I30N, were created on Cx26 gene by site-directed mutagenesis. In order to create mutations on Cx26 gene 5'- and 3'- fragments were produced by use of primers with single nucleotide changes in PCR reactions. Then, mutant full-length Cx26 fragments were produced in PCR reaction by use of the previously produced 5'- and 3'- fragments as templates. Primers in Table 2.1 were used to create each mutation in the products of three-step PCR reaction as described below

- A88V Mutation

Firstly, pBSBK-Cx26 vector was used as template DNA with 5'Cx26 and A88V reverse primers to produce 287 bp fragment with A88V mutation at 5' fragment. Secondly, A88V forward and 3'Cx26 primers were used in PCR reaction with pBSBK-Cx26 vector to produce 418 bp fragment with A88V mutation at 3' fragment. Finally, 287 bp and 418 bp fragments were used as a template with 5'Cx26 and 3'Cx26 primers to produce 705 bp Cx26A88V fragment (Figure 3.1).

- D50A Mutation

In the first PCR reaction, pBSBK-Cx26 vector was used as a template DNA with 5'Cx26 and D50A reverse primers and 172 bp fragment with D50A mutation at 5' fragment was produced. Secondly, D50A forward and 3'Cx26 primers were used with pBSBK-Cx26 vector to produce 558 bp fragment with D50A mutation at 3' fragment. Finally, 172 bp and 558 bp fragments were used as a template with 5'Cx26 and 3'Cx26 primers to produce 705 bp Cx26D50A fragment (Figure 3.2).

- D50Y Mutation

Firstly, pBSBK-Cx26 vector was used as a template DNA with 5'Cx26 and D50Y reverse primers to produce 172 bp fragment with D50Y mutation at 5' fragment. Then, D50Y forward and 3'Cx26 primers were used in the second PCR reaction with pBSBK-Cx26 vector to produce 558 bp fragment with D50Y mutation at 3' fragment.

Finally, 172 bp and 558 bp fragments were used as a template with 5'Cx26 and 3'Cx26 primers to produce 705 bp Cx26D50Y fragment (Figure 3.2).

- I30N Mutation

Initially, pBSBK-Cx26 vector was used as a template DNA with 5'Cx26 and I30N reverse primers to produce 115 bp fragment with I30N mutation at 5' fragment. I30N forward and 3'Cx26 primers were used in the second PCR reaction with pBSBK-Cx26 vector to produce 617 bp fragment I30N mutation at 3' fragment. Finally, 115 bp and 617 bp fragments were used as a template with 5'Cx26 and 3'Cx26 primers to produce 705 bp Cx26I30N fragment (Figure 3.1).

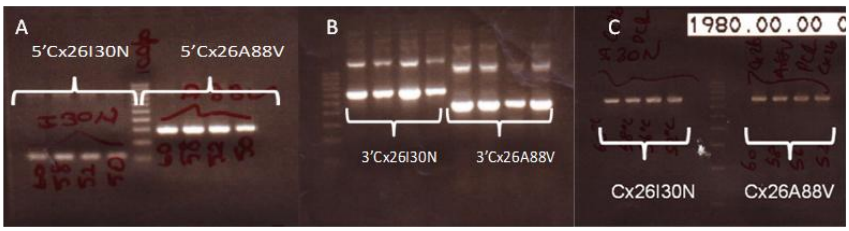

Figure 3.1. Cloning of Cx26A88V and Cx26I30N fragments A) 115 bp 5'Cx26I30N and 287 bp 5'Cx26A88V fragments were produced as 1st PCR products for Cx26I30N and A88V mutants, respectively. B) 617 bp 3'Cx26I30N and 418 bp 3'Cx26A88V fragments were produced in the 2nd PCR reactions for Cx26I30N and A88V mutants, respectively. C) 705 bp Cx26I30N and Cx26A88V fragments were produced as final PCR products by using the corresponding 1st and 2nd PCR products as template DNA.

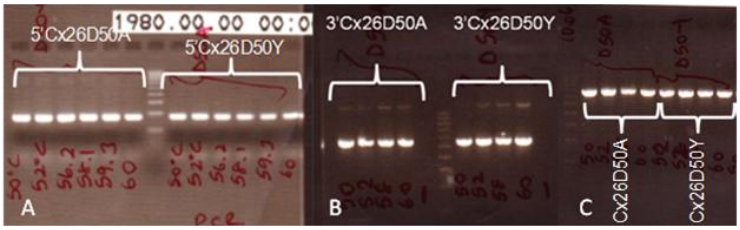

Figure 3.2. Cloning of Cx26D50A and Cx26D50Y fragments A) 172 bp 5'Cx26D50A and 5'Cx26D50Y fragments were produced as 1st PCR products for Cx26D50A and D50Y clones, respectively. B) 548 bp 3'Cx26D50A and 3'Cx26D50Y fragments were produced as 2nd PCR products. C) 705 bp Cx26D50A and Cx26D50Y fragments were produced as final PCR products by using the corresponding 1st and 2nd PCR products as a template DNA.

Produced PCR products were cloned into pBSBK vector and sent to Macrogen Inc. for sequencing. Then by using MultAlin Multiple sequence alignment by Florence Corpet (http://multalin.toulouse.inra.fr/multalin/multalin.html) program they were compared to the normal Cx26 sequence. Sequencing results showed that A88V (Figure

3.3A), D50A (Figure 3.3B), D50Y (Figure 3.3C) ve I30N (Figure 3.3D) mutations on Cx26 were perfectly created at the correct locations (Figure 3.3).

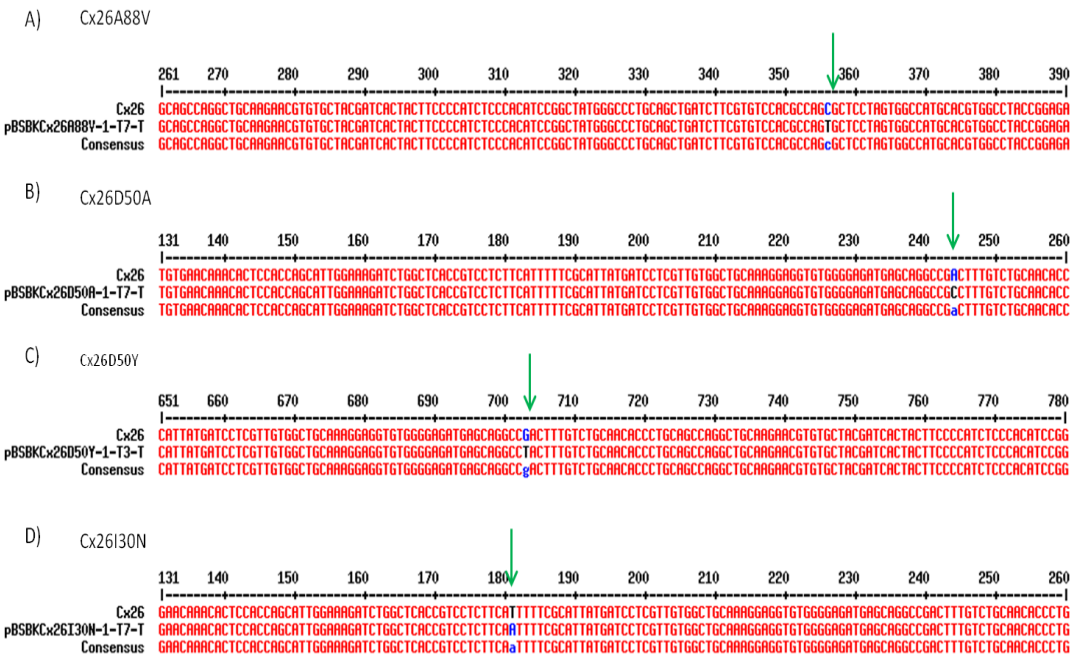

Figure 3.3. A part of sequence comparison with Cx26 WT and mutants: Sequencing results that show perfect matches with normal Cx26 sequence except the mutations at the correct locations shown with arrows. A) 5'- and 3'- Cx26A88V with 263C>T, B) 5'- and 3'- Cx26D50A with 149A>C, C) 5'- and 3'- Cx26D50Y with 148G>T, D) 5'- and 3'- Cx26I30N with 89T>A mutations.

3.2. Transfection of pIRES2-EGFP and pIRES2-DsRed2 constructs into N2A and HeLa cells

N2A and HeLa cells are gap junctional communication-deficient cell lines so they are widely used to examine the functions of gap junctions. That is why we also used these cell lines in our studies and also this way, we can study the properties of mutant channels. At the beginning, transfection of pIRES2-EGFP and pIRES2-DsRed2 constructs were optimized with cells in 24-well plate with different ratio combinations of DNA and Lipofectamine 2000. As a result, transfection of pIRES2-EGFP and pIRES2-DsRed2 constructs into N2A and HeLa cells were optimized with a ratio of 1:2 DNA(µg):Lipofectamine(µl) reagent, respectively. Transfection efficiency was higher in N2A cells compared to HeLa cells when controlled under a fluorescent microscope (Figure 3.4). Therefore, for dye uptake and expression studies N2A cells were used.

However, HeLa cells are more widespread and larger than N2A cells so they were prefered for immunostaining experiments to determine the localization of mutant Cx26 proteins. Moreover, the transfection efficiency was higher when pIRES2-EGFP constructs were used rather than pIRES2-DsRed2 constructs. Therefore, pIRES2-EGFP constructs were used for transfection in our experiments.

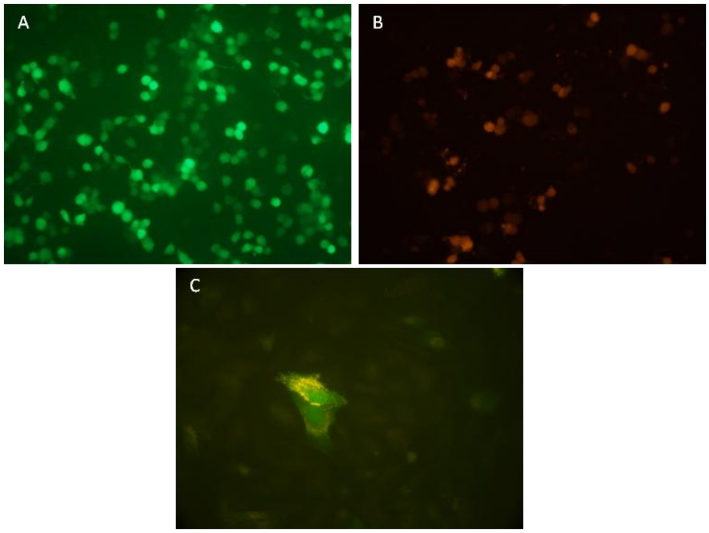

Figure 3.4. Transfection of constructs into N2A and HeLa cells. A) N2A cells that were transfected with pIRES2-EGFP Cx26 WT. B) N2A cells transfected with pIRES2-DsRed2 Cx26 WT. C) HeLa cells transfected with pIRES2-EGFP Cx26 WT shown as an example for comparison of the transfection efficiency.

3.3. Immunohistochemistry of Cx26 in HeLa cells

Mutations on Cx26 could affect the intracellular localization of the protein. Therefore, the effect of mutations on the protein localization was compared with Cx26 WT in HeLa cells transfected with pIRES2-EGFP constructs using immunohistochemistry with primary rabbit anti-Cx26 antibody and Alexa555-conjugated goat anti rabbit secondary antibody. They were also stained with DAPI to determine the locations of nuclei of the cells. In wild type condition connexins were observed to be localized in both cytoplasm and plasma membrane. However, in mutant conditions, proteins were mainly observed to be localized in the cytoplasm and no gap junction plaques were observed between adjacent cells. In Cx26A88V mutant condition, less viable cells were observed when compared to other conditions after transfection (Figure 3.5 and Figure 3.6).

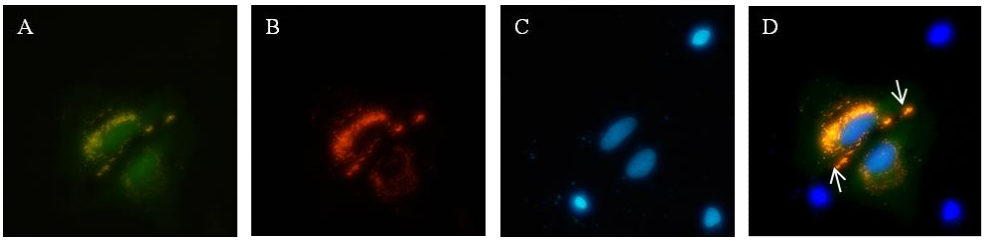

Figure 3.5. Immunostaining of Hela cells with normal Cx26. A) HeLa cells transfected with pIRES2-EGFP Cx26 WT (green). B) Immuno-stained HeLa cells with secondary antibody (Alexa555) (red) shows the localization of Cx26 proteins. C) DAPI-stained HeLa cells. D) Merged image of HeLa cells with fluorescence of EGFP, secondary antibody (Alexa555) and DAPI. Yellow color is caused by merged color of transfected cells (green) and Cx26 proteins (red). Arrows show the gap junction plaques between adjacent cells

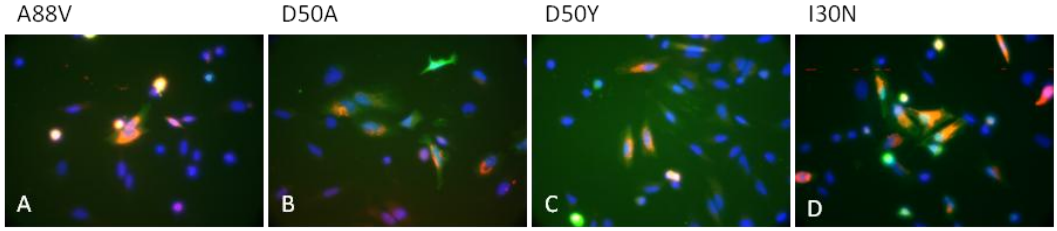

Figure 3.6. Merged images of HeLa cells transfected with pIRES-EGFP (green) constructs. A) pIRES2-EGFP Cx26A88V, B) pIRES2-EGFP Cx26D50A, C) pIRES2-EGFP Cx26D50Y, D) pIRES2-EGFP Cx26I30N. Red color shows the Cx26 proteins' localization. Yellow color is the merged color of transfected cells (green) and Cx26 proteins (red).

3.4. Western Blot

Mutations in Cx26 could interfere with the protein expression of Cx26 protein. In order to control expression of proteins and determine if A88V, D50A, D50Y and I30N mutations have any effect on the protein level, Western blot analysis was done on transfected cells to compare the expression levels of mutant proteins with Cx26 WT. In order to do that, pIRES2-EGFP Cx26 WT and mutant vectors were transfected into N2A cells. After Western blotting, both wild type and mutant human Cx26 proteins expressed in N2A cells were observed at 26 kDa. Cx26 WT protein had the highest expression level compared to mutant proteins. The expression levels of Cx26D50A and Cx26D50Y were close to each other. Cx26A88V condition showed little expression. However, Cx26I30N condition showed no significant expression and was similar to negative control, pIRES2-EGFP expressing cells. Loading amounts were observed

approximately the same for all conditions by comparing the expression of mouse housekeeping protein γ-tubulin that was observed at 46 kDa (Figure 3.7, top panel).

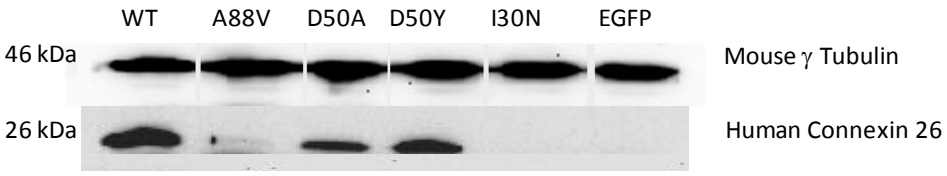

Figure 3.7. Western blotting: Cx26 expression was observed in pIRES2-EGFP Cx26 WT, pIRES2-EGFP Cx26D50A, pIRES2-EGFP-D50Y lanes, observed in pIRES2-EGFP Cx26A88V lane in small amounts. And it could not be observed in pIRES2-EGFP Cx26I30N lane. pIRES2-EGFP empty vector was used as a negative control.

Analysis of Western blot images was done by dividing the density of Cx26 bands to the density of γ-tubulin bands and calculating averages of three replicates of Western blot experiments (Figure-3.8). Student's t-test was used to compare the protein amount of each mutation with Cx26 WT expression (n=3). In Figure 3.8 expression of Cx26 WT is significantly ($p<0.05$) higher than mutant Cx26 expressions. Cx26D50A and Cx26D50Y expression levels were similar to each other. The expression of Cx26I30N protein could not be observed.

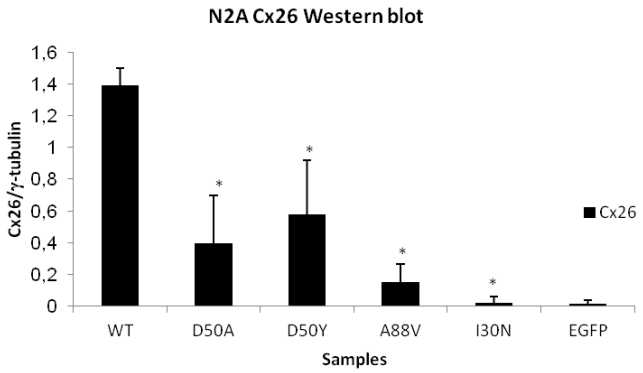

Figure 3.8. Analysis of Western blotting: Cx26 expression graph in both wild type and mutant conditions as an average of three replicates (*:$p<0.05$).

3.5. RT-PCR of Cx26 in N2A cells

A change in the protein expression, might be due to a problem in mRNA expression. Therefore, RT-PCR analysis of transfected N2A cells was performed to compare the expression levels of Cx26 WT and mutant conditions at the mRNA level. In order to do that pIRES2-EGFP Cx26 WT and mutant constructs were transfected into

N2A cells and RT-PCR analysis for Cx26 was performed with Cx26 primers and control, mouse housekeeping gene (GAPDH), primers (Figure 3.9). Student's t-test was used to compare the mRNA amount of each mutant condition with Cx26 WT. The expression of Cx26 WT is significantly ($p<0.05$) lower than Cx26D50A, Cx26D50Y and Cx26I30N conditions. However, the expression of Cx26A88V was not statistically different from Cx26 WT ($p>0.05$).

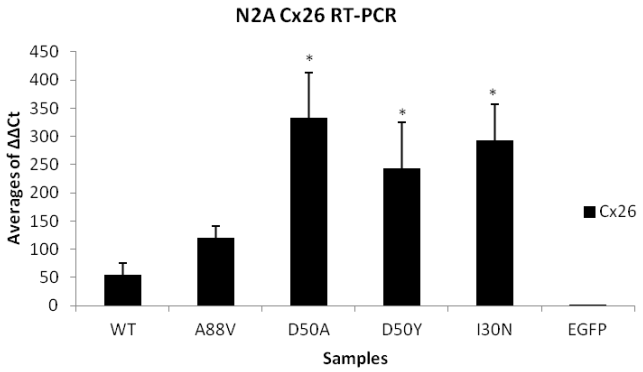

Figure 3.9. Cx26 RT-PCR in N2A cells: Expression of Cx26 gene in wild type and mutant Cx26 expressing cells. (*:$p<0.05$)

3.6. Ethidium Bromide uptake in N2A cells

Mutations on connexins could also alter the function of hemichannels and/or gap junction channels. In order to determine the hemichannel activities of mutant Cx26 proteins; N2A cells were transfected with pIRES2-EGFP Cx26 WT and mutant constructs (Figure 3.10). After that EtBr (MW 394 Da, charge +1) uptake assay was performed together with pIRES2-EGFP Cx26A40V mutant that was shown to have leaky hemichannels *in vitro* (Montgomery et al., 2004) (Figure 3.11). Here, untransfected cells and empty vector (pIRES2-EGFP) transfected cells were used as negavite controls. The transfer of EtBr from the extracellular environment into the cell through mutant channels was analyzed on ImageJ program (http://rsbweb.nih.gov/ij/) by using images taken with the fluorescent microscope. As seen in figure 3.11; there was a significant increase in dye uptake through mutant hemichannels compared to the Cx26 WT and negative controls, pIRES2-EGFP empty vector transfected and untransfected cells ($p<0.05$). Furthermore, mutations had similar dye uptake capacity with the positive control, Cx26A40V hemichannels ($p>0.05$).

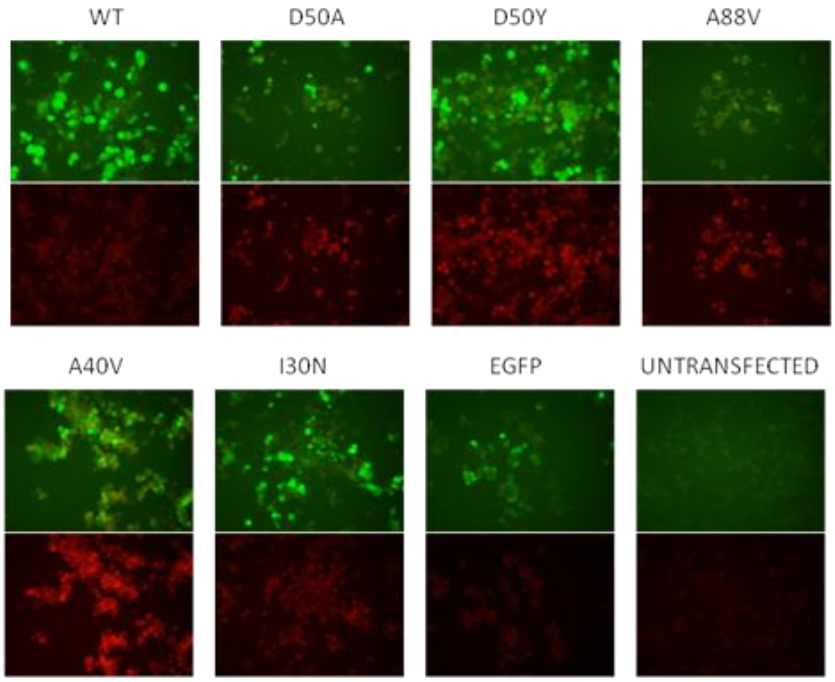

Figure 3.10. EtBr uptake: Wild type and mutant Cx26 transfected cells with the proved mutation, CxA40V and negative controls, pIRES2-EGFP transfected and untransfected cells. Top panels are the images of EGFP (green) transfected N2A cells, and bottom panels are the images of the N2A cells that uptake EtBr (red).

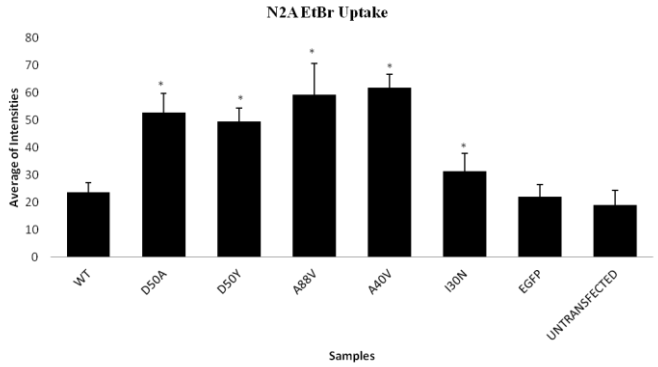

Figure 3.11. Analysis of EtBr uptake: Wild type and mutant Cx26 transfected cells with the proved mutation, Cx26A40V and negative controls, pIRES2-EGFP transfected and untransfected cells. (*:$p<0.05$)

3.7. Neurobiotin uptake in N2A cells

In order to further examine the hemichannel activity of mutant Cx26 channels, a smaller molecule than EtBr, Neurobiotin (NB, MW 287 Da, charge +1) was used in dye

uptake assays (Figure 3.12). N2A cells were transfected with pIRES2-EGFP Cx26 WT and mutant constructs and NB uptake assay was performed with the proved mutation, pIRES2-EGFP Cx26A40V as a positive control and negative controls, pIRES2-EGFP transfected and untransfected cells (Figure 3.13). Mutations Cx26D50A, Cx26D50Y, Cx26A88V and Cx26I30N had NB transfer from extracellular environment into the cell much more than Cx26 WT ($p<0.05$). Moreover, NB uptake capacity of Cx26D50A, Cx26D50Y, Cx26A88V and Cx26I30N transfected cells was significantly higher than negative controls ($p<0.05$), pIRES2-EGFP empty vector transfected and untransfected cells and it was also similar with the capacity of Cx26A40V hemichannels ($p>0.05$).

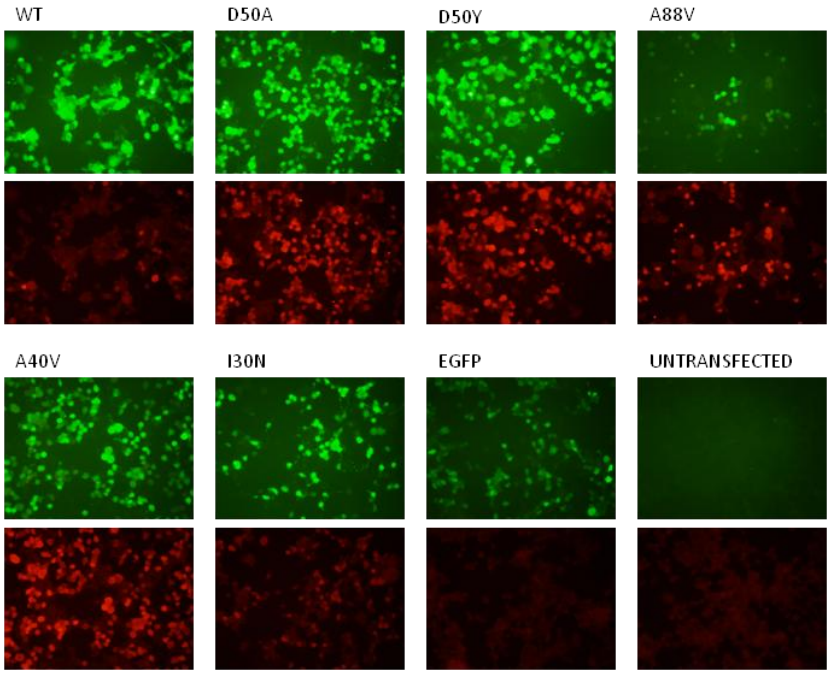

Figure 3.12. NB uptake: Wild type and mutant Cx26 transfected cells with the proved mutation, Cx26A40V and negative controls, pIRES2-EGFP transfected and untransfected cells. Top panels are the images of EGFP (green) transfected N2A cells, and bottom panels are the images of N2A cells that uptake NB (red).

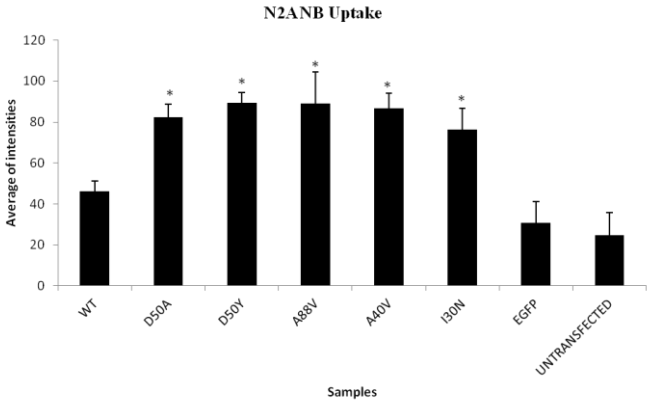

Figure 3.13. Analysis of NB uptake: Cells transfected with pIRES2-EGFP Cx26 WT and mutant constructs (*:$p<0.05$)

3.8. Lucifer Yellow uptake in N2A cells

In addition to EtBr and NB uptake assays, an anionic fluorescent molecule, Lucifer yellow (LY, MW 433 Da, charge -2) was also used in dye uptake assay on transfected cells. Since LY is observed green under fluorescent microscope, N2A cells were transfected with wild type and mutant pIRES2-DsRed2 Cx26 constructs. On the following day, LY uptake assay was performed with negative controls pIRES2-DsRed2 transfected and untransfected cells (Figure 3.14). Lucifer yellow uptake assay was repeated five times and only worked once. Therefore, statistical analysis could not be done.

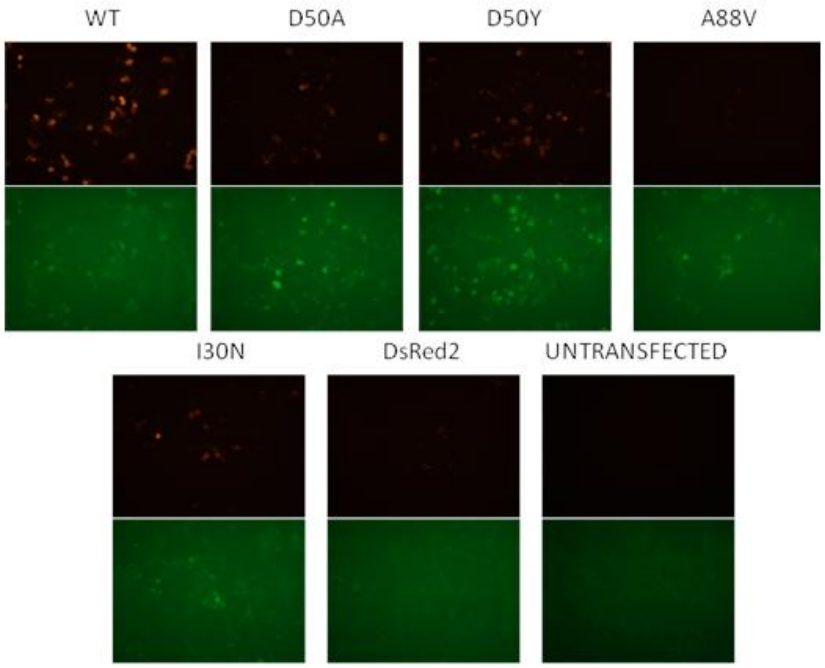

Figure 3.14. LY uptake: Wild type and mutant Cx26 transfected cells with negative controls pIRES2-EGFP transfected and untransfected cells. Top panels are the images of DsRed (red) transfected N2A cells, and bottom panels are the images of N2A cells that uptake LY (green).

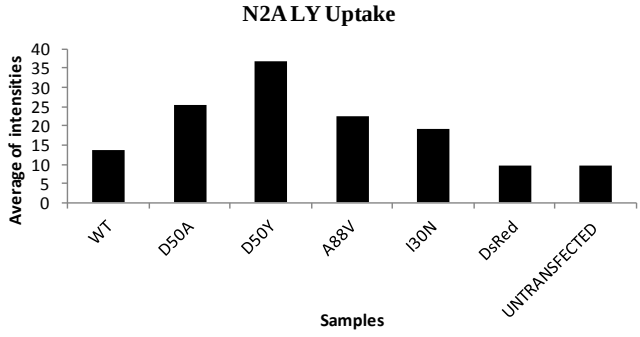

Figure 3.15. Analysis of LY uptake: N2A cells transfected with pIRES2-EGFP Cx26 wild type and mutant constructs

3.9. RT-PCR of Cx26 and Keratin10 in HaCaT cells

In order to understand the effect of Cx26 mutations on keratinocyte physiology, an immortalized keratinocyte cell line, HaCaT, was used to study these mutations. Initially, RT-PCR analysis of Keratin 10 expression was performed on pIRES2-EGFP wild type and mutant Cx26 transfected HaCaT cells to investigate the effect of Cx26

mutations on the differentiation of keratinocytes. Keratin 10 is one of the biomarkers of keratinocytes at the suprabasal layers of epidermis. RT-PCR analysis was performed with Cx26, Keratin 10 and control, human GAPDH, primers. We observed that there was no significant changes on Keratin 10 expression dependent on Cx26 wild type and mutant conditions ($p>0.05$, $n=3$). In addition, only the expression of Cx26I30N was significantly higher than Cx26 WT ($p<0.05$). Other conditions including negative control, pIRES2-EGFP, were statistically similar to Cx26 WT ($p>005$) (Figure 3.16).

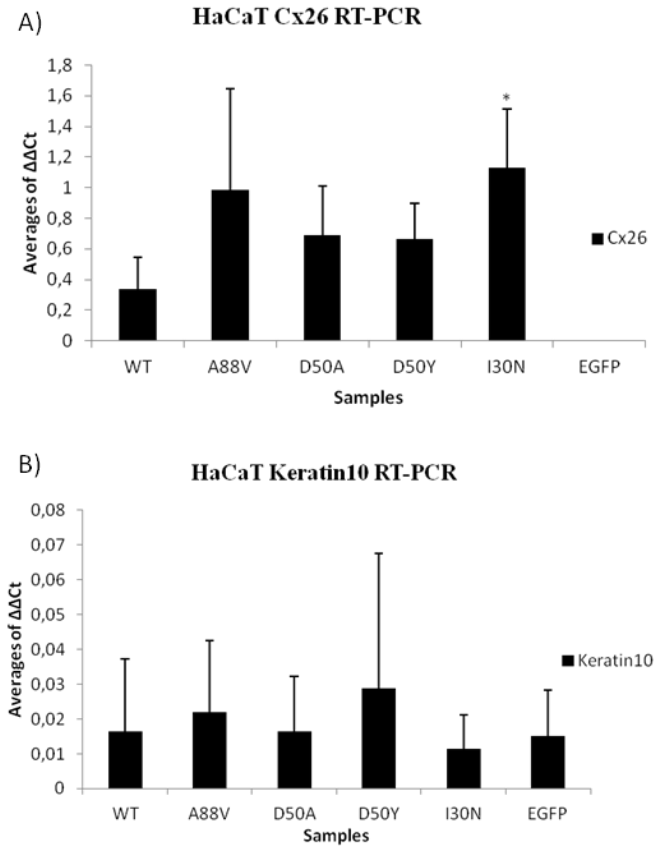

Figure 3.16. Effect of Cx26 mutants on Keratin 10 expression in HaCaT cells: A) Cx26 expression in HaCaT cells. B) Keratin 10 expression in HaCaT cells.

CHAPTER 4

DISCUSSION

Mutations in Cx26 result in hearing loss and skin disorders. Various types of pathologies could come up from different single nucleotide changes in the same gene and this proves us that unique channel activities could occur in mutation (Mhaske et al., 2013). For Keratitis-Ichthyosis-Deafness (KID) syndrome mutations Cx26-G12R (Lee et al., 2009), Cx26-N14K (Zwart-Storm et al., 2010), Cx26-A40V (Montgomery et al., 2004), Cx26-G45E (Meşe et al., 2011), and Cx26-D50N (Richard et al., 2002) were observed to have increased hemichannel activity. Most of the mutations on Cx26 that cause hearing loss were characterized; however, the number of characterized skin disorder-associated mutations is much less, relatively.

In our study we have selected four uncharacterized novel mutations; A88V (Koppelhus et al., 2010), D50A (Cushing et al., 2008), D50Y (Yotsumoto et al., 2003), I30N (Arndt et al., 2010) which were detected in patients with KID syndrome. Selected mutations were created with site-directed mutagenesis in Cx26 cDNA. Then, functions of these mutations were tested in HeLa and N2A which are gap junctional communication-deficient cell lines and in immortalized human keratinocyte cell line, HaCaT which has endogenously expressed Cx26.

CHAPTER 5

CONCLUSION

Localization of wild type and mutant Cx26 proteins was detected with immunohistochemistry in Hela cells. Immunostaining of Cx26 showed that wild type proteins could be observed in both cytoplasm and plasma membrane. However, there was no observation of mutant connexins, forming gap junction plaques between adjacent cells as wild type. Thus, they were only observed to be localized in cytoplasm. In addition to that, Mhaske et al. also could not observe clear localization at plasma membrane for Cx26A88V and Cx26D50A (Mhaske et al., 2013).

In Western blot, expression of mutant Cx26 proteins was significantly lower than normal, Cx26 WT condition. For Cx26I30N condition there was no significant protein expression. However, in RT-PCR experiments Cx26 WT mRNA level was notably lower than mRNA level of mutant ones except Cx26A88V. This conflict could be explained as mutant proteins might be less stable than wild type proteins or when Cx26 is mutated its folding might change and Cx26 antibody could not bind to it properly, thus protein expression could not be observed in Western blotting for some of the mutant proteins. However, immunostaining experiments showed that there was expression of Cx26I30N similar to other mutations. The stability of mutant proteins could further be investigated by PoPMuSiC v2.1 (http://babylone.ulb.ac.be/popmusic/) or similar bioinformatical programs that can evaluate the stability changes of a given protein or peptide in the presence of single-site mutation.

Dye uptake assays were performed in communication deficient cell lines to test if any of the mutants has increased hemichannel activity compared to Cx26 WT channels. In dye uptake assays EtBr, NB and LY were used. In EtBr and NB uptake assays, A88V, D50A, D50Y and I30N mutants were observed to form leaky hemichannels. Similar to our observations, it was recently demonstrated that D50A and A88V mutations cause increased hemichannel activity in *Xenopus* oocytes using electrophysiological measurements (Mhaske et al., 2013). Furthermore, Mhaske et al. found that A88V was lethal for cRNA-injected *Xenopus*-oocytes. We also made similar observations in our experiments; when we transfected N2A cells, Hela cells and keratinocytes with Cx26 A88V mutant, the number of cell death was higher than Cx26

WT and other mutants after the transfection. However, the mechanism is not known and further cell death assays should be performed to prove cell death.

In the structure of connexins, transmembrane domain 3(TM3) is assumed to form the lining of the channel. TM1, N-terminal and first extracellular loop were shown to be associated with the voltage sensor of the channel. When this voltage sensor moves it functions in gating of the channel and this movement is provided by distortion in TM2 by a conserved proline. The experiments of removal of proline had been shown to cause reversal in the open and closed states of the channel (Yeager and Nicholson, 1996). Moreover, created mutations on Cx26 can cause structural deformities that occur by different properties of altered amino acids. For I30N mutation, isoleucine (I) is a hydrophobic amino acid and asparagine (N) is a hydrophilic amino acid and this alteration can lead to twists in TM1. For both D50A and D50Y mutations, aspartate (D) is a hydrophilic amino acid, and alanine (A) and tyrosine (Y) are both hydrophobic amino acids that can cause structural changes in the first extracellular loop. For A88V mutation, both alanine (A) and valine (V) are hydrophobic amino acids and there may not be an important structural change in TM2 and overall connexin structure. (http://www.mcb.ucdavis.edu/courses/bis102/aaprop.html)

Although KID syndrome is caused by mutations in the same gene, each mutation cause different phenotypes and that may show different mutations can have different effects on keratinocyte differentiation. Differentiation of keratinocytes can be checked by expression of epidermal biomarkers two of which are keratin 1 and keratin 10; biomarkers for suprabasal layers (Pommerencke et al., 2008). In addition, keratin 1 with keratin 10 form keratin intermediate filaments which provide strength and flexibility to epidermis (Fuchs et al., 1992). In our study, HaCaT cells were transfected with wild type and mutant constructs to understand the effect of Cx26 mutants on keratinocytes. RT-PCR analysis demonstrated that Keratin 10 expression was not affected by Cx26 expression in both wild type and mutant conditions. Thus, selected mutations could be said to have no effect on the differentiation of keratinocytes.

In conclusion, we have found that KID syndrome associated A88V, D50A, D50Y and I30N mutations on Cx26 have increased hemichannel activity compared to wild type Cx26. It needs further research to determine if these mutations lead to release of important cytoplasmic molecules such as ATP into the extracellular space. Moreover, A88V mutation was observed to cause less transfected cells for three different cell

types. Therefore, further experiments such as apoptosis test could be performed to find the mechanism of this case.

REFERENCES

Arndt, S., Aschendorff, A., Schild, C., Beck, R., Maier, W., Laszig, R., & Birkenha, R. (2010). A Novel Dominant and a De Novo Mutation in the GJB2 Gene (Connexin-26) Cause Keratitis-Ichthyosis-Deafness Syndrome : Implication for Cochlear Implantation, 210–215.

Article, R. (2000). Connexins : a connection with the skin, 77–96.

Bevans, C. G., Kordel, M., Rhee, S. K., & Harris, A. L. (1998). Isoform Composition of Connexin Channels Determines Selectivity among Second Messengers and Uncharged Molecules *, *273*(5), 2808–2816.

Biology, C. (2004). Genetic Heterogeneity of KID Syndrome : Identification of a Cx30 Gene (GJB6) Mutation in a Patient with KID Syndrome and Congenital Atrichia, 1108–1113.

Cushing, S. L., Macdonald, L., Propst, E. J., Sharma, A., Stockley, T., Blaser, S. L., James, A. L., et al. (2008). Successful cochlear implantation in a child with Keratosis , Icthiosis and Deafness (KID) Syndrome and Dandy-Walker malformation, 1–6. doi:10.1016/j.ijporl.2008.01.017

Desche, S. M., Walcott, J. L., Wexler, T. L., Scherer, S. S., & Fischbeck, K. H. (1997). Altered Trafficking of Mutant Connexin32, *17*(23), 9077–9084.

Du, Á., Mesnil, M., & Yamasaki, H. (1997). Dominant-negative abrogation of connexin-mediated cell growth control by mutant connexin genes.

Eckert, R., Traub, O., & Hiilser, D. E. (1995). Specific Permeability and Selective Formation of Gap Junction Channels in Connexin-transfected HeLa Cells, *129*(3), 805–817.

Fuchs, E., Esteves, R. A., & Coulombet, P. A. (1992). Transgenic mice expressing a mutant keratin 10 gene reveal the likely genetic basis for epidermolytic hyperkeratosis, *89*(August), 6906–6910.

Gemel, J., Valiunas, V., Brink, P. R., & Beyer, E. C. (2004). Connexin43 and connexin26 form gap junctions , but not heteromeric channels in co-expressing cells. doi:10.1242/jcs.01084

Gerido, D. A., Derosa, A. M., Richard, G., & White, T. W. (2013). Aberrant hemichannel properties of Cx26 mutations causing skin disease and deafness Aberrant hemichannel properties of Cx26 mutations causing skin disease and deafness, (April 2007). doi:10.1152/ajpcell.00626.2006

Gerido, D. A., & White, T. W. (2004). Connexin disorders of the ear , skin , and lens, *1662*, 159–170. doi:10.1016/j.bbamem.2003.10.017

Goldberg, G. S., Moreno, A. P., & Lampe, P. D. (2002). Gap Junctions between Cells Expressing Connexin 43 or 32 Show Inverse Permselectivity to Adenosine and ATP *, *277*(39), 36725–36730. doi:10.1074/jbc.M109797200

Goldberg, G. S., Valiunas, V., & Brink, P. R. (2004). Selective permeability of gap junction channels, *1662*, 96–101. doi:10.1016/j.bbamem.2003.11.022

Goodenough, D. A., & Paul, D. L. (2009). Gap Junctions, 1–19. doi:10.1101/cshperspect.a002576

Holmes, D., Clavin, W., Harrison, M. R., & Adzick, N. S. (1997). The human homeobox genes MSX-1 , MSX-2 , and MOX-1 are differentially expressed in the dermis and epidermis in fetal and adult skin. *Differentiation*, *62*(1), 33–41. doi:10.1046/j.1432-0436.1997.6210033.x

Kelsell, D. P., Di, W., & Houseman, M. J. (2001). Connexin Mutations in Skin Disease and Hearing Loss, *26*(Mim 124500), 559–568.

Koppelhus, U., Tranebjærg, L., Esberg, G., Ramsing, M., Lodahl, M., & Rendtorff, N. D. (2010). A novel mutation in the connexin 26 gene (GJB2) in a child with clinical and histological features of keratitis – ichthyosis – deafness (KID) syndrome, 142–148. doi:10.1111/j.1365-2230.2010.03936.x

Koval, M. (2006). Pathways and control of connexin oligomerization, *16*(3). doi:10.1016/j.tcb.2006.01.006

Laird, D. W. (2005). Connexin phosphorylation as a regulatory event linked to gap junction internalization and degradation, *1711*, 172–182. doi:10.1016/j.bbamem.2004.09.009

Laird, D. W. (2009). The gap junction proteome and its relationship to disease, (November). doi:10.1016/j.tcb.2009.11.001

Lee, J. R., Derosa, A. M., & White, T. W. (2009). Connexin Mutations Causing Skin Disease and Deafness Increase Hemichannel Activity and Cell Death when Expressed in Xenopus Oocytes, *129*. doi:10.1038/jid.2008.335

Lee, J. R., & White, T. W. (2009). Connexin-26 mutations in deafness and skin disease, *11*(November), 1–19. doi:10.1017/S1462399409001276

Marziano, N. K., Casalotti, S. O., Portelli, A. E., Becker, D. L., & Forge, A. (2003). Mutations in the gene for connexin 26 (GJB2) that cause hearing loss have a dominant negative effect on connexin 30, *12*(8), 805–812. doi:10.1093/hmg/ddg076

Mese, G., Sellitto, C., Li, L., Wang, H., & Valiunas, V. (2011). The Cx26-G45E mutation displays increased hemichannel activity in a mouse model of the lethal form of keratitis-ichthyosis-deafness syndrome, *2*. doi:10.1091/mbc.E11-09-0778

Mhaske, P. V, Levit, N. A., Li, L., Wang, H., Lee, J. R., Shuja, Z., Brink, P. R., et al. (2013). The human Cx26-d50a and Cx26-A88V mutations causing keratitis-ichthyosis-deafness syndrome display increased hemichannel activity, *8661*, 1–9. doi:10.1152/ajpcell.00374.2012

Montgomery, C. J. R., White, T. W., Martin, B. L., Turner, M. L., & Holland, S. M. (2004). A novel connexin 26 gene mutation associated with features of the keratitis-ichthyosis-deafness syndrome and the follicular occlusion triad, 377–382. doi:10.1016/j.jaad.2003.12.042

Niessen, H., Harz, H., Bedner, P., Krämer, K., Willecke, K., Genetik, I., Molekulargenetik, A., et al. (2000). Selective permeability of different connexin channels to the second, *1372*, 1365–1372.

Papers, J. B. C., Doi, M., Musil, L. S., Le, A. N., Vanslyke, J. K., & Roberts, L. M. (2000). Regulation of Connexin Degradation as a Mechanism to Increase Gap Junction Assembly and Function *, *275*(33), 25207–25215. doi:10.1074/jbc.M002608200

Pommerencke, T., Steinberg, T., Dickhaus, H., Tomakidi, P., & Grabe, N. (2008). Nuclear staining and relative distance for quantifying epidermal differentiation in biomarker expression profiling. *BMC bioinformatics*, *9*, 473. doi:10.1186/1471-2105-9-473

Reaction, R. T. C. (2008). Connexin Expression and Functional Analysis of Gap Junctional Communication in Mouse Embryonic Stem Cells AND, 431–439. doi:10.1634/stemcells.2007-0482

Richard, G., & White, T. W. (2007). Gap Junctions : Basic Structure and Function, *127*(December 2006), 2516–2524. doi:10.1038/sj.jid.5700770

Sánchez, H. A., Me, G., Srinivas, M., White, T. W., & Verselis, V. K. (2010). Differentially altered Ca 2 + regulation and Ca 2 + permeability in Cx26 hemichannels formed by the A40V and G45E mutations that cause keratitis ichthyosis deafness syndrome, 47–62. doi:10.1085/jgp.201010433

Scott, C. A., & Kelsell, D. P. (2011). Key functions for gap junctions in skin and hearing, *254*, 245–254. doi:10.1042/BJ20110278

Segretain, D., & Falk, M. M. (2004). Regulation of connexin biosynthesis , assembly , gap junction formation , and removal, *1662*, 3–21. doi:10.1016/j.bbamem.2004.01.007

Tattersall, D., Scott, C. A., Gray, C., Zicha, D., & Kelsell, D. P. (2009). EKV mutant connexin 31 associated cell death is mediated by ER stress, *18*(24), 4734–4745. doi:10.1093/hmg/ddp436

Titeux, M. (2009). Keratitis-Ichthyosis-Deafness Syndrome Caused by GJB2 Maternal Mosaicism, *129*. doi:10.1038/jid.2008.312

White, T. W., & Paul, D. L. (1999). GENETIC DISEASES AND GENE KNOCKOUTS REVEAL DIVERSE CONNEXIN FUNCTIONS, 283–310.

Yeager, M., & Nicholson, B. J. (1996). Structure of gap junction intercellular channels. *Current opinion in structural biology*, *6*(2), 183–92. Retrieved from http://www.ncbi.nlm.nih.gov/pubmed/8728651

Yotsumoto, S., Hashiguchi, T., Chen, X., Ohtake, N., & Tomitaka, A. (2003). Cutaneous Biology Novel mutations in GJB2 encoding connexin-26 in Japanese patients with keratitis – ichthyosis – deafness syndrome, 649–653.

Zoidl, G., & Dermietzel, R. (2010). Gap junctions in inherited human disease. doi:10.1007/s00424-010-0789-1

Zwart-storm, E. A. De, Rosa, R. F. M., Martin, P. E., Foelster-holst, R., Frank, J., Bau, A. E. K., Zen, P. R. G., et al. (2010). Molecular analysis of connexin26 asparagine14 mutations associated with syndromic skin phenotypes, 408–412. doi:10.1111/j.1600-0625.2010.01222.x